PHYSICAL REVIEW B **89**, 235204 (2014)

Photon assisted tunneling in pairs of silicon donors

K. L. Litvinenko,[1,*] S. G. Pavlov,[2] H.-W. Hübers,[2,3] N. V. Abrosimov,[4] C. R. Pidgeon,[5] and B. N. Murdin[1]

[1]*Advanced Technology Institute, University of Surrey, Guildford GU2 7XH, United Kingdom*

[2]*Institute of Planetary Research, German Aerospace Center (DLR), Ruthefordstraße 2, 12489 Berlin, Germany*

[3]*Technische Universität Berlin, Institut für Optik und Atomare Physik, Hardenbergstraße 36, 10623 Berlin, Germany*

[4]*Leibniz Institute for Crystal Growth, Berlin, Germany*

[5]*Institute of Photonics and Quantum Science, SUPA, Heriot-Watt University, Edinburgh EH14 4AS, United Kingdom*

(Received 12 May 2014; revised manuscript received 4 June 2014; published 19 June 2014)

Shallow donors in silicon are favorable candidates for the implementation of solid-state quantum computer architectures because of the promising combination of atomiclike coherence properties and scalability from the semiconductor manufacturing industry. Quantum processing schemes require (among other things) controlled information transfer for readout. Here we demonstrate controlled electron tunneling at 10 K from P to Sb impurities and vice versa with the assistance of resonant terahertz photons.

DOI: 10.1103/PhysRevB.89.235204 PACS number(s): 03.67.Lx, 71.55.Cn, 72.25.−b, 78.47.D−

I. INTRODUCTION

The implementation of many of the building blocks of a solid-state quantum computer still remains challenging. In the original Kane proposal [1], logical operations on individual spins and spin readout measurements are performed by means of electric fields externally applied to donor atoms in silicon. For readout, spin information may be transferred from a single donor electron or nucleus to the charge degree of freedom via spin-dependent tunneling from a single qubit donor to a single electron transistor (SET) island, and this has been demonstrated experimentally [2]. Spin-to-charge conversion between a qubit donor and a readout donor (as opposed to a readout island) has the advantage that it is much more exactly scalable [3]. In this case a SET is still required to sense the charge state of the readout donor, but it does not have to be connected as closely for charge sensing as for spin sensing. Tunneling from a 1s neutral donor to a 1s neutral donor can be represented as $D_{1s}D_{1s} \rightarrow D^+D^-$ where the final state is sometimes called a charge-transfer state or a donor exciton. The lowest-energy final state is only possible when both electrons have different spins. This process requires a relatively strong external dc electric field in order to overcome the energy difference between the $D_{1s}D_{1s}$ and D^+D^- states [3]. Unfortunately the electric field is so large that it causes field ionization of the D^+D^- state. One of the proposed solutions to reduce the dc field was to apply an additional ac electric field with a frequency resonantly tuned to the energy difference between the $D_{1s}D_{1s}$ and D^+D^- states. The binding energy of the D^+D^- state is found to be inversely proportional to the distance between the adjacent atoms because the presence of the Coulomb interaction between the charged donors stabilizes it [3,4], and for a donor separation of 20–40 nm lies between the energy of the $2p_0$ and $2p_\pm$ states of an isolated donor [5]. The frequency required is therefore about 10 THz, which can be produced with far-infrared (FIR) radiation from an off-chip source. It has been shown theoretically [5] that resonant photons can, in principle, produce very significant reduction of the electric field required for tunneling to the charge-transfer (SET) atom, which is enough to fulfill the requirements for the adiabatic SET spin readout in the Kane scheme, and that the donor separation should be more than 30 nm; otherwise backward transitions ($D_{1s}D_{1s} \rightarrow D^-D^+$ rather than $D_{1s}D_{1s} \rightarrow D^+D^-$) and intradonor excitations dominate.

In optical transmission experiments where backward transitions are not important, the $D_{1s}D_{1s} \rightarrow D^+D^-$ absorption is visible in randomly doped samples with densities from 2 to 20 $\times$ 10^{16} cm^{-3}. It appears as an apparent asymmetric broadening of the isolated donor $D_{1s} \rightarrow D_{F2p}$ lines [4,6]. For densities below 10^{16} cm^{-3} isolated D^- ions (with binding energy of the order of few meV) may be visible in photoconductivity, though a significant fraction of the negative donor ions are formed as negatively charged D_2^- pairs [7], while at higher donor concentrations, the charge-transfer state becomes an impurity conduction band [7]. The $D_{1s}D_{1s} \rightarrow D^+D^-$ has not therefore been observed at densities low enough for significant numbers of pairs with separation above 30 nm.

In this work we investigate the charge-transfer dynamics using the pump-probe technique, i.e., the transient absorption produced by short, intense THz pulses. In this experiment, the absorption of the probe is sensitive to the difference in population between the ground and excited states; a short pump pulse causes an instantaneous repopulation detected by the probe pulse. The recovery of the probe transmission is recorded as a function of the time delay between the pulses. For silicon doped by group V elements with low density the technique has been used to determine the intracenter relaxation times which typically lie in the range of 100–300 ps [8–10].

II. DISTRIBUTION OF PAIR SEPARATIONS

The distribution of nearest-neighbor distances for random doping is shown for different concentrations in Fig. 1. The minimum doping for observation of $D_{1s}D_{1s} \rightarrow D^+D^-$ in the small-signal transmission, 2×10^{16} cm^{-3} [6], produces a narrow distribution of pair spacings between about 10–30 nm. To have a majority of donors with separation greater than 30 nm (and so avoid the backwards transitions) requires a density of about 4×10^{15} cm^{-3} or less. At this density it can be seen that an eighth of the impurities have a neighbor close enough for

*Corresponding author: k.litvinenko@surrey.ac.uk

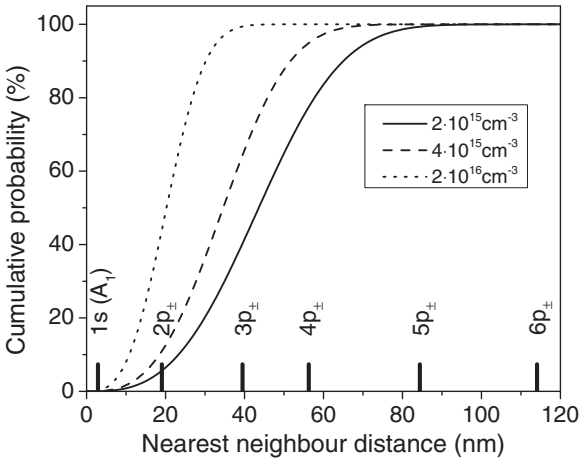

FIG. 1. For a Poisson distribution, the probability that there are no donors in a volume V is e^{-nV}, so the cumulative probability that there are other donors within radius r from one impurity of interest is just $1–\exp(–4\pi nr^3/3)$, where the lines shown are for different values of n. Hence 98.5% of impurities have a neighbor within a distance $n^{-1/3}$. (It also follows that the probability density function for the interdonor distance is $4\pi r^2 n \exp(–4\pi nr^3/3)$ per unit radius and the expected interdonor distance is $\langle r\rangle = 0.554n^{-1/3}$.) Also indicated along the abscissa are the center-to-center distances for touching orbitals (i.e., the Bohr diameters) found by scaling the binding energies [11].

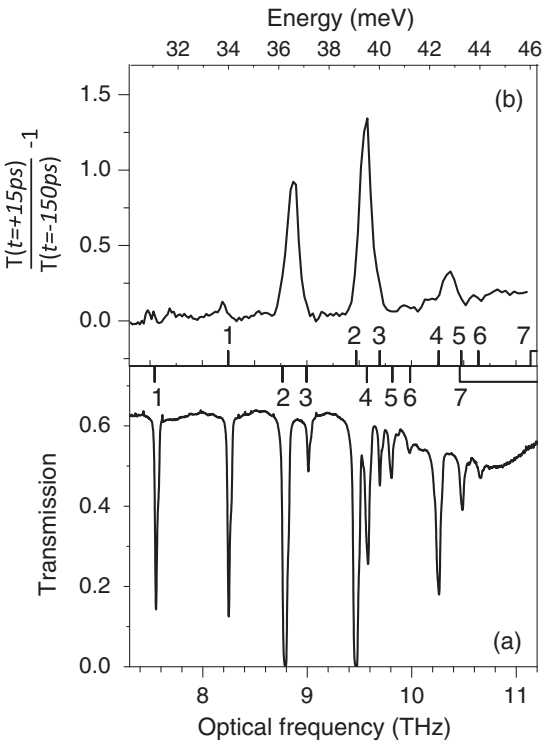

FIG. 2. Small-signal (a) and nonequilibrium (b) transmission spectroscopy of the codoped silicon sample. Transition energies [12] are labeled according to the excited state (all originating from the $1s(A_1)$ ground state) for (a) antimony and (b) phosphorus (1-2p_0, 2-2$p_\pm$, 3-3p_0, 4-3$p_\pm$, 5-4$p_\pm$, 6-5$p_\pm$, and 7-conduction band). In (a) the transmission signal at 4.2 K has been normalized to the instrument response. In (b) the differential transmission of the probe at 10 K is shown at fixed delay between probe and pump pulses of +15 ps (pumped), normalized with the signal at −150 ps (unpumped).

the Bohr radii of the $2p_\pm$ orbitals to touch, and the distribution peaks (steepest rise in the cumulative distribution) at 40 nm. In this paper we report the observation of the dynamics by resonant THz pumping in samples with a total donor density of $3–4\times10^{15}$ cm^{-3}.

In order to produce a high fraction of excited donors we used intense pump pulses, and to further ensure that a high fraction of the excited donors have unexcited neighbors, we used two different impurity species (P, Sb) for the pumped (qubit) and charge-transfer (readout) donor atoms. The ground states of the group V donors have different energy because they have different arrangement of electrons and potentials in the central unit cell at the donor site. On the other hand, effective mass theory predicts that the odd-parity excited states are the same for all species (the local differences are irrelevant because the wave function is zero near the central cell for an odd-parity state) and can be calculated by simple scaling of the hydrogen excited states, taking into account the dielectric constant and the effective electron mass in silicon [12,13]. The excited states and therefore the resonant tunneling are identical in homodonor (P-P and Sb-Sb) and heterodonor pairs (P-Sb). The variation of the ground-state energies of different donor atoms results only in an energy shift of the optical transitions, which means that it is possible to pump a specific species by THz frequency selection (Fig. 2). The sample has nearly equal numbers of each species so half of the nearest-neighbor pairs are heterodonor pairs, and in these pairs if one species of the donors is excited optically the other one will remain in the ground state. The same material has previously been used for realization of multifrequency terahertz lasing under optical pumping [14], and as expected for this concentration, no evidence of broadening of the absorption and emission lines due to pair complexes was seen.

III. EXPERIMENTAL METHODS

All silicon crystals (see Table I) used in this study were grown by the float zone technique with simultaneous doping from the melt. For the codoped sample, the primary source material was a phosphorus-doped silicon crystal with a donor concentration of 1.8×10^{15} cm^{-3} and compensation below 1%. Antimony was added to the source material by a subsequent pedestal growth procedure. As a control we examined single species samples with the same total density ($\sim$3–4$\times10^{15}$ cm^{-3}) of either P or Sb, in which case photon assisted tunneling is inhibited because of the equal THz excitation of both components in a pair.

The small-signal transmission spectrum of the codoped sample at 4.2 K is shown in Fig. 2(a). All phosphorus and antimony transitions up to the $5p_\pm$ states are clearly resolved. The energy positions of absorption transitions are exactly the same as for monodoped Si:Sb and Si:P crystals (data not shown) and the linewidths of the transitions (0.9 cm^{-1}) are comparable with Si:P and Si:Sb linewidths.

The samples were mounted in vacuum on the same cold finger of a liquid helium cryostat with polypropylene film windows. The sample temperature was estimated to be about 10 K, well above the sensor reading of 5 K because of blackbody radiation through the window. The samples

TABLE I. Silicon samples used in this study.

Sample No.	Dopant	Concentration, (10^{15}cm^{-3})	Dimensions thickness x (large facet)	Orientation to large facets[a]
V2682	P	4.0	$1.0 \times (7.0 \times 7.0)$ mm^3	[100]
V473	Sb	3.8	$1.0 \times (10.2 \times 10.0)$ mm^3	[111]
	P	1.8		
V496			$0.5 \times (10.0 \times 10.0)$ mm^3	[100]
	Sb	1.2		

[a]The large facets of the samples are chemically-mechanically polished and wedged with ∼1°.

were therefore mounted in pairs [Si:(P,Sb) with Si:P; and subsequently Si:(P,Sb) with Si:Sb], to produce exactly the same experimental conditions in the investigation of each pair, choosing one or the other sample by a vertical translation of the cold finger. A free-electron laser (FELIX, then at the FOM Institute for Plasma Physics "Rijnhuizen," Nieuwegein, the Netherlands) was used as a source of ultrashort coherent pulse with 2-μJ pulse energy and the pulse length of <10 ps. The laser was focussed to a spot of a millimeter diameter and the intensity adjusted so that the pump excitation was about 50% (i.e., the pump pulse area was $\pi/2$ [15]). The pulse repetition time was 40 ns in a 4-μs burst. The probe pulse was taken from the same beam using a pellicle beam splitter, and the effect of shot noise was reduced by balancing the detection with a reference pulse, an identical copy of the probe, arriving 20 ns later and hence unaffected by the pump [9].

IV. RESULTS AND DISCUSSION

In order to investigate the resonant nature of the pump-probe excitation and to estimate the strength of the nonlinear signals, first we fixed a positive delay (pump before probe) of 15 ps (where the amplitude of the pump-induced change in the probe transmission is almost maximal) and scanned the FELIX wavelength over the whole spectral range of interest. The recorded spectrum was then normalized by a similar spectrum taken at −150 ps negative delay (probe arrives before pump), which represented the unbleached probe transmission. The results are shown in Fig. 2(b). The $1s$ to $2p_0$, $2p_\pm$, and $3p_\pm$ donor transitions are clearly recognizable for all the samples. The observed linewidths of the transitions are broader than those in small signal due to finite linewidth of the bandwidth-limited FELIX pulses.

The dynamics of the photoexcited electrons may be adequately described by a three-level rate equation system (ground state, excited state, and continuum) [8]. Ignoring the relaxation from the continuum into the excited state (applicable for sufficiently low temperatures), and ignoring multiphoton ionization (if the intensity is not too high), and assuming that the ionization occurs within first few tens of picoseconds, the recovery of the probe transmission is proportional to [8]

$$\Delta T(t) \sim \Delta T_x E^{-t/T_1} + \Delta T_i \left(1 - \frac{t}{t + t_R}\right), \qquad (1)$$

where $\Delta T_{x,i}$ is the initial probe transmission change due to occupation of the excited state and the continuum, respectively, and the former gives rise to exponential decays while the latter produces reciprocal decay. T_1 is the relaxation time, and t_R is the initial, concentration-dependent, ion recombination time.

The recovery of the pump-induced transmission of the probe beam as a function of the time delay between pump and probe beams is shown in Fig. 3 for excitation from the phosphorus $1s(A_1)$ ground state (P_{1s}) to the continuum in Si:P. As expected, pumping directly into the continuum produces reciprocal recovery corresponding to $T_x = 0$ in Eq. (1). The initial ion recombination time is extracted to be $t_R = 65$ ps, which differs only slightly from the value estimated in Ref. [8] because of the different initial pumped concentration. Excitation to the continuum for the other two samples (not shown) was also found to produce reciprocal decay with comparable values of t_R. The $D_{1s} \rightarrow D_{3p\pm}$ transitions in Si:P and Si:Sb samples also exhibit reciprocal recovery (not shown) suggesting that thermal ionization occurs when the excited state (binding energy 3.1 meV in this case) is shallow and approaches $k_B T$ (0.9 meV at 10 K).

The pump-probe transient was measured for the pairs of samples under the same resonant excitation conditions for transitions to all the $2p$ states except the $Sb_{1s} \rightarrow Sb_{2p0}$, and is shown in Fig. 4. The signal-to-noise ratio of the $Sb_{1s} \rightarrow Sb_{2p0}$ transition was not enough to perform the measurement (as can be seen from the signal size at 7.1 THz in Fig. 2). The relaxation of the electrons from the $2p$ is well described by a single exponential decay in the monodoped samples, with characteristic times that agree very well with our previous results [8–10]. No reciprocal decay component was seen, indicating thermal ionization from the excited state is

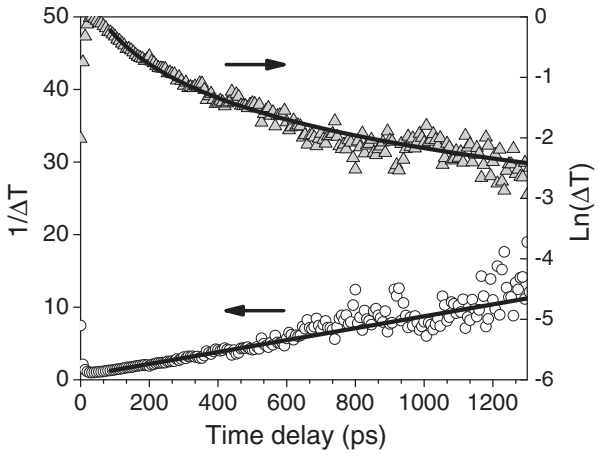

FIG. 3. The logarithm and reciprocal of normalized ΔT, the change in probe transmission due to the pump, as a function of the delay between the pulses. The excitation was directly from P_{1s} into the continuum at 11.1 THz. The transmission recovery is well described by reciprocal decay (with $t_R = 65$ ps) as can be seen from the linear relationship between $1/\Delta T$ and delay.

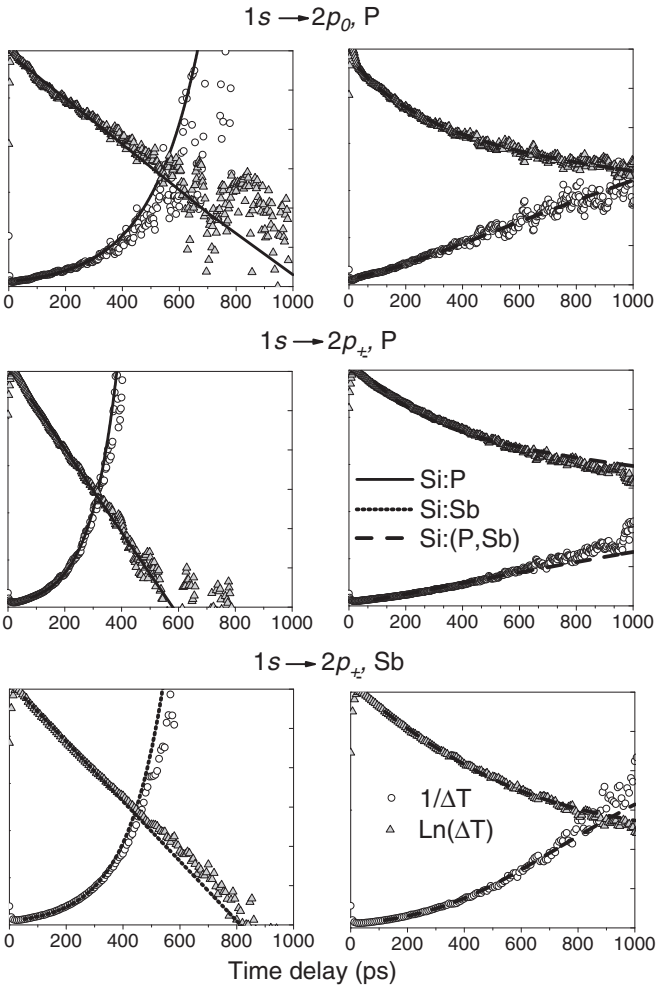

FIG. 4. As Fig. 3 for different samples and resonant transitions as labeled. Every panel has the same axes, and the ticks on the right-hand ordinate are integer steps in $\ln(\Delta T)$. For each experiment on the codoped sample (right column) the same transition was measured in the corresponding monodoped sample (left column) with identical conditions. The monodoped samples are well described by single exponential decays with the following relaxation times: $1s \rightarrow 2p_0$, P: $T_1 = 175$ ps; $1s \rightarrow 2p_\pm$, P: $T_1 = 95$ ps; $1s \rightarrow 2p_\pm$, Sb: $T_1 = 135$ ps. For the codoped sample the recovery was fitted with both components: $1s \rightarrow 2p_0$, P: $T_1 = 142$ ps, $t_R = 70$ ps; $1s \rightarrow 2p_\pm$, P: $T_1 = 100$ ps, $t_R = 64$ ps; $1s \rightarrow 2p_\pm$, Sb: $T_1 = 166$ ps, $t_R = 67$ ps.

negligible under the temperature and intensity conditions used due to the competition with the direct relaxation pathway. In the codoped sample the dynamics cannot be reproduced with a single exponential decay. Fitting the relaxation with a sum of exponential and reciprocal components according to Eq. (1) produces a lifetime for the exponential component that is very similar to the equivalent monodoped sample transition, giving confidence in the fit. The existence of a reciprocal component in the recovery of the $P_{1s} \rightarrow P_{2p\pm}$ transition in the Si:(P,Sb) sample might be explained by its spectral overlap with $Sb_{1s} \rightarrow Sb_{3p\pm}$ transition (see Fig. 2), which is therefore simultaneously pumped. As already mentioned the $3p_\pm$ level is susceptible to thermal ionization and the measured overall transient reflects the separate contribution of each of them, so the dynamics is a complicated mix of direct relaxation in the P- and Sb-related ionization and recombination. On the other hand, there is no such spectral overlap of $P_{1s} \rightarrow P_{2p0}$ and $Sb_{1s} \rightarrow Sb_{2p\pm}$ transitions with any other allowed transitions in the codoped sample, other than the $D_{1s}D_{1s} \rightarrow D^+D^-$. Clearly, in the codoped sample the charge-transfer state is involved in the process, and it is responsible for the appearance of an extra reciprocal component in the recovery of the probe transmission. The charge-transfer state has a long lifetime due to the significant suppression of backwards transitions by the low doping concentration, and thermal ionization occurs before return or relaxation. The long, reciprocal decay component is only apparent after exponential decay of over a decade, meaning that a relatively small fraction of the donors (<10%) undergo the charge transfer, i.e., the branching ratio with the direct relaxation is low.

Figure 2 shows that the process is strongly resonant, and must involve intradonor excitation initially, i.e., $D_{1s}D_{1s} \rightarrow D_{2p}D_{1s} \rightarrow D^+D^-$. We note that the charge-transfer states resonant with $2p_\pm$ have donor separation of 40 nm while those resonant with $2p_0$ have separation about 20 nm [5]. The direct excitation to the charge-transfer state is much weaker, corresponding to the background signal off resonance on Fig. 2 because it is spread out in energy, and only those pairs aligned along the electric field vector of the light beam can be excited. It would be interesting to investigate this further with a means of probing the excitation that does not rely on the transmission changes, such as by electrical pump-pump experiments [16]. It would also be interesting to probe the temperature dependence to determine the ionization energy of the relevant charge-transfer states, and this is the subject of future work.

It is important to remember that the small-signal spectrum of the codoped sample shows lines with widths that are just as narrow as the lines for the monodoped material, and typical for natural silicon hosts. These lines are inhomogeneously broadened, due to the random arrangement of silicon isotopes around the impurity, which affects the potential because the amplitude of the zero-point fluctuations depends on mass. There is no evidence that the crystal quality of the codoped sample is any different from the monodoped material, and therefore there are no additional competing effects of dislocations, etc. As already mentioned the samples were mounted in pairs so the experimental conditions were identical. In summary, the only difference between the codoped sample relative to the monodoped sample of the same density is the higher probability of unexcited neighbors for the former.

V. CONCLUSION

We have shown here that the tunneling between phosphorus and antimony atoms occurs even at zero external electric fields and can be controlled by selective photoexcitation of either phosphorus or antimony atoms. The effect of the tunneling was detected through its longer hold time in the excited state and the consequent increase in the thermal ionization compared with samples with reduced charge-transfer state creation. We note that in applications reducing the temperature for quantum computing readout schemes [3] would be used to make thermal ionization improbable. We also note that it is possible to reduce the tunneling by reducing the donor spacing [5], as in the donor molecules important for another quantum gating scheme [17].

In the latter application tunneling of the photoexcited electron is not required, and the spacing of the atoms is about 10 nm. Our results show that the spin-to-charge conversion (which would be possible if an external magnetic field were added) is perfectly feasible with photon assisted tunneling, as required for Kane-type quantum computing schemes.

ACKNOWLEDGMENTS

We gratefully acknowledge the support of the EPSRC-UK (COMPASSS, Grant No. EP/H026622), and FOM-NL in providing the required beam time on FELIX. B.N.M. is grateful for a Royal Society Wolfson Research Merit Award.

[1] B. E. Kane, Nature **393**, 133 (1998).
[2] F. A. Zwanenburg, A. S. Dzurak, A. Morello, M. Y. Simmons, L. C. L. Hollenberg, G. Klimeck, S. Rogge, C. N. Coppersmith, and M. A. Eriksson, Rev. Mod. Phys. **85**, 961 (2013).
[3] L. C. L. Hollenberg, C. J. Wellard, C. I. Pakes, and A. G. Fowler, Phys. Rev. B **69**, 233301 (2004).
[4] M. Capizzi, G. A. Thomas, F. DeRosa, R. N. Bhatt, and T. M. Rice, Solid State Commun. **31**, 611 (1979).
[5] M. J. Testolin, A. D. Greentree, C. J. Wellard, and L. C. L. Hollenberg, Phys. Rev. B **72**, 195325 (2005).
[6] G. A. Thomas, M. Capizzi, F. DeRosa, R. N. Bhatt, and T. M. Rice, Phys. Rev. B **23**, 5472 (1981).
[7] P. Norton, J. Appl. Phys. **47**, 308 (1976).
[8] N. Q. Vinh, P. T. Greenland, K. Litvinenko, B. Redlich, A. F. G. van der Meer, S. A. Lynch, M. Warner, A. M. Stoneham, G. Aeppli, D. J. Paul, C. R. Pidgeon, and B. N. Murdin, Proc. Natl. Acad. Sci. USA **105**, 10649 (2008).
[9] N. Q. Vinh, B. Redlich, A. F. G. van der Meer, C. R. Pidgeon, P. T. Greenland, S. A. Lynch, G. Aeppli, and B. N. Murdin, Phys. Rev. X **3**, 011019 (2013).
[10] H.-W. Hübers, S. G. Pavlov, S. A. Lynch, Th. Greenland, K. L. Litvinenko, B. Murdin, B. Redlich, A. F. G. van der Meer, H. Riemann, N. V. Abrosimov, P. Becker, H.-J. Pohl, R. Kh. Zhukavin, and V. N. Shastin, Phys. Rev. B **88**, 035201 (2013).
[11] R. G. Pires, R. M. Dickstein, S. L. Titcomb, and R. L. Anderson, Cryogenics **30**, 1064 (1990).
[12] A. K. Ramdas and S. Rodriguez, Rep. Prog. Phys. **44**, 1297 (1981).
[13] B. N. Murdin, J. Li, M. L. Y. Pang, E. T. Bowyer, K. L. Litvinenko, S. K. Clowes, H. Engelkamp, C. R. Pidgeon, I. Galbraith, N. V. Abrosimov, H. Riemann, S. G. Pavlov, H.-W. Hübers, and P. G. Murdin, Nat. Commun. **4**, 1469 (2013).
[14] S. G. Pavlov, R. Eichholz, N. V. Abrosimov, B. Redlich, and H.-W. Hübers, Appl. Phys. Lett. **98**, 061102 (2011).
[15] P. T. Greenland, S. A. Lynch, A. F. G. van der Meer, B. N. Murdin, C. R. Pidgeon, B. Redlich, N. Q. Vinh, and G. Aeppli, Nature **465**, 1057 (2010).
[16] E. T. Bowyer, B. J. Villis, Juerong Li, K. L. Litvinenko, B. N. Murdin, M. Erfani, G. Matmon, G. Aeppli, J.-M. Ortega, R. Prazeres, Li Dong, and Xiaomei Yu. [Appl. Phys. Lett. (to be published)] (2014).
[17] A. M. Stoneham, A. J. Fisher, and P. T. Greenland, J. Phys.: Condens. Matter **15**, L447 (2003).